Enhancing Distribution Network Resilience: A Hierarchical Collaborative Optimization Method Considering Steel Plant Demand Response and SOP

Jiawei Qu, Danyang Xu, Kai Hou, Zeyu Liu*, Hongjie Jia
State Key Laboratory of Smart Power Distribution Equipment and System
Tianjin University
Tianjin, China
{jiawei_qu, danyangxu, khou, tjulzy, hjjia}@tju.edu.cn

Abstract—**In recent years, the frequency and intensity of extreme natural disasters have increased, placing significant impact on the resilience of distribution networks. To address this challenge, demand-side management combined with soft open points (SOP) has emerged as an important strategy to enhance resilience. This paper proposes a hierarchical collaborative optimization model that integrates steel plant demand response (SPDR) and SOP to improve the resilience of distribution networks under extreme weather events. This model is formulated as a bilevel mixed-integer linear programming (BMILP) problem. Furthermore, a mixed-integer L-shaped method (MIL-shaped) is developed to efficiently solve this problem. A case study demonstrates that the collaborative optimization of steel plant demand response and SOP significantly enhances the resilience of the distribution network against both topology-damaging and load-shocking disasters. Numerical results show that the MIL-shaped method not only improves the system's robustness to extreme natural disasters but also significantly enhances computational efficiency.**

Index Terms—resilience enhancement, distribution network, hierarchical collaborative optimization, soft open points, steel plant.

I. Introduction

The frequency and intensity of extreme natural disasters, such as floods, typhoons, and heatwaves, have been steadily increasing, posing significant challenges to the resilience of distribution networks (DNs) [1]. These events disrupt the normal operation of power systems, leading to increased risks of load shedding, equipment damage, and power outages. DNs are becoming increasingly vulnerable to these extreme conditions, highlighting the urgent need for resilience-enhancing strategies to maintain reliability.

Several strategies have been proposed to enhance the resilience of distribution networks during extreme natural disasters, with demand-side management (DSM) emerging as a key approach. DSM provides a flexible method for adjusting load during peak demand periods to mitigate load shedding caused by extreme cold, heat, and other events. Among these, industrial demand response, particularly in energy-intensive sectors such as steel plants, offers greater potential for resilience enhancement due to their large and relatively predictable loads. However, the DSM strategy cannot improve resilience in topology-damaging scenarios. When combined with soft open points (SOP), steel plants can act as flexible points for rerouting power flow, significantly improving the reliability.

In [2], a coordinated scheduling method for energy-intensive industries and thermal power generation is proposed to reduce peak load and enhance the operational reliability of the power system. A multi-timescale scheduling method that incorporates industrial loads and energy storage is proposed in [3], employing stochastic optimization to achieve resilient system operation. In addition, a resilience-oriented SOP deployment model that considers various islanding operation states under post-fault scenarios is developed in [4]. In [5], a coordinated reconfiguration method for SOPs is presented to realize resilience restoration across different electrical subsystems and an adaptive ADMM-based distributed solution approach is adopted to address the proposed model. However, research on the coordinated enhancement of system resilience through the joint flexibility of industrial loads and SOPs remains lacking.

To address the above-mentioned issue, this paper proposes a hierarchical collaborative optimization model that integrates steel plant demand response (SPDR) and soft open points (SOP) to enhance the resilience of distribution networks under various extreme disaster conditions. This model is formulated as a bilevel mixed-integer linear programming (BMILP) model, in which the upper-level master problem captures the optimal demand-response decisions of steel plants, while the lower-level subproblem minimizes load shedding of the distribution network. Considering that a single region may be affected by multiple types of extreme weather events, a unified climate impact model is developed. The proposed optimization problem is solved using a mixed-integer L-shaped (MIL-shaped) method. Furthermore, to overcome the limitation of the traditional L-shaped method,

This work was supported by the Smart- Grid·National Science and Technology·Major·Project (No. 2025ZD0806300).

979-8-3315-8138-1

which can only solve linear subproblems, this study extends the L-shaped approach [6] to handle subproblems containing integer variables, providing a mixed-integer formulation for optimality cuts The main contributions are as follows,

1) A hierarchical collaborative optimization model is proposed integrating steel plant demand response (SPDR) and soft open points (SOP) to enhance distribution network resilience under extreme conditions.

2) A unified climate impact model has been developed to assess the impact of various extreme natural disasters on the distribution system.

3) An extended MIL-shaped algorithm capable of efficiently solving mixed-integer subproblems by introducing a mixed-integer formulation for optimality cuts.

II. HIERARCHICAL COLLABORATIVE OPTIMIZATION MODEL

This section provides the detailed formulation of the hierarchical collaborative optimization model, as illustrated in Fig. 1. Fig. 2 depicts the steel plant structure, comprising the coking, electric arc furnace (EAF), sintering, pelletizing, blast furnace (BF), basic oxygen furnace (BOF), and rolling processes. In the hierarchical collaborative optimization model, the upper-level master problem aims to minimize the total system cost, including operation costs associated with steel plants and load shedding cost, thus achieving optimal demand response decisions for the steel plant. The lower-level subproblem employs robust optimization to determine the minimum load shedding cost of the distribution network under the worst-case extreme natural disaster scenarios.

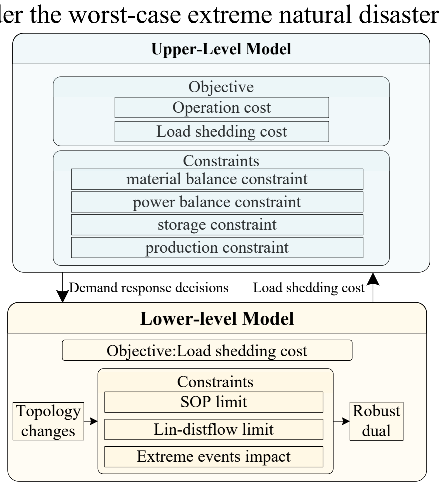

Figure 1. The hierarchical collaborative optimization model

A. Upper-level model

1) Objective function

The objective of the upper-level problem is to minimize the operation cost of steel plants and the load shedding cost of the distribution system.

$$\min C_{\text{all}} = C_{\text{op}} + C_{\text{rel}} \tag{1}$$

where C_{op} and C_{rel} are the operation cost and load shedding cost, respectively. C_{op} is determined by the electricity consumption cost of each process, as shown in (2), whereas C_{rel} is obtained through operational simulations of the distribution network using the lower-level model.

$$C_{\text{dr}} = \sum_t p_t^{\text{ele}} \cdot P_t^{\text{steel}} \tag{2}$$

where t denotes the time index, and k denotes the process index. p_t^{ele} denotes the electricity price. P_t^{steel} represents the total power of steel plant at time t.

2) Constraints

Based on process characteristics, steel production can be divided into continuous and non-continuous production processes. The continuous production processes include sintering, pelletizing, BF, BOF, and rolling, and the production models are formulated as follows:

$$P_k^{\text{con,min}} \le P_{k,t}^{\text{con}} \le P_k^{\text{con,max}} \tag{3}$$

$$S_k^{\text{con,min}} \le S_{k,t}^{\text{con}} \le S_k^{\text{con,max}} \tag{4}$$

$$S_{k,t}^{\text{con}} = S_{k,t\text{-}1}^{\text{con}} + \rho_{k,t}^{\text{con}} P_{k,t}^{\text{con}} - \sum_{j \in \Omega_k} P_{j,t}^{\text{con}} \tag{5}$$

where $P_{k,t}^{\text{con}}$ represents the power of continuous process k at time t, with $P_k^{\text{con,min}}$ and $P_k^{\text{con,max}}$ denoting the minimum and maximum power limits of continuous production process k, respectively. $S_{k,t}^{\text{con}}$ indicates the material storage level of continuous process k at time t, bounded by minimum and maximum storage capacities $S_k^{\text{con,min}}$ and $S_k^{\text{con,max}}$, respectively. $\rho_{k,t}^{\text{con}}$ represents the continuous production per unit of electricity for process k, and Ω_k denotes the set of downstream processes associated with process k. j is the index of downstream processes.

The non-continuous production processes include coking and EAF, with their production models formulated as follows:

$$y_{k,t}^{\text{ucon}} - y_{k,t\text{-}1}^{\text{ucon}} = srt_{k,t}^{\text{ucon}} - srt_{k,t\text{-}1}^{\text{ucon}} \tag{6}$$

$$\sum_t srt_{k,t}^{\text{ucon}} = 1 \tag{7}$$

$$S_{k,t}^{\text{ucon}} = S_{k,t\text{-}1}^{\text{ucon}} + \rho_{k,t}^{\text{ucon}} P_{k,t}^{\text{ucon}} - \sum_{j \in \Omega_k} P_{j,t}^{\text{ucon}} \tag{8}$$

$$P_k^{\text{ucon,min}} y_{k,t}^{\text{ucon}} \le P_{k,t}^{\text{ucon}} \le P_k^{\text{ucon,max}} y_{k,t}^{\text{ucon}} \tag{9}$$

where the binary state variable $y_{k,t}^{\text{ucon}}$ represents the operational state of non-continuous process k, with 1 indicating that the process is active. $srt_{k,t}^{\text{ucon}}$ denotes the start-up or shutdown status, with 1 representing that the process is starting. $P_{k,t}^{\text{ucon}}$ represents the power of non-continuous process k at time t, with $P_k^{\text{ucon,min}}$ and $P_k^{\text{ucon,max}}$ denoting the minimum and maximum power limits of non-continuous production process k, respectively. $S_{k,t}^{\text{ucon}}$ indicates the material storage level of non-continuous process k at time t, bounded by minimum and maximum storage capacities $S_k^{\text{ucon,min}}$ and $S_k^{\text{ucon,max}}$, respectively. $\rho_{k,t}^{\text{ucon}}$ represents the non-continuous production per unit of electricity for process k. (7) specifies that within a daily production cycle, a production unit k can be started at most once.

In summary, the total power of the steel plant can be expressed as follows:

$$P_t^{\text{steel}} = \sum_k P_{k,t}^{\text{con}} + P_{k,t}^{\text{ucon}} \tag{10}$$

979-8-3315-8138-1

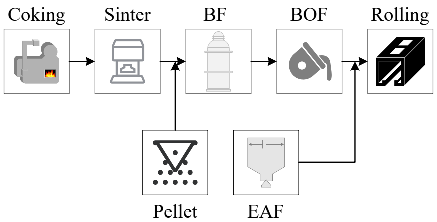

Figure 2. The structure of steel plants

B. Lower-level model

1) Objective function

The objective function of the lower-level model is to minimize load shedding costs through the fewest switching operations.

$$C_{\mathrm{rel}} = \sum_{s\in\Omega_s} p_s \Big(\sum_{j\in\Omega_n} \gamma^{\mathrm{ls}} P_{s,j}^{\mathrm{ls}} + \sum_{sw\in\Omega_{\mathrm{sw}}} \gamma^{\mathrm{sw}} N_{s,sw} \Big) \tag{11}$$

where s denotes the scenario index, j denotes the node index, and sw denotes the switch index. Ω_s, Ω_n, and Ω_{sw} represent the extreme weather events set, system nodes set, and switches set, respectively. p_s is the probability of scenario s. γ^{ls} denotes the unit cost of load shedding, and γ^{sw} denotes the cost associated with switching operations. $P_{s,j}^{\mathrm{ls}}$ denotes the load shedding at node j, and $N_{s,sw}$ denotes the number of switching operations.

2) Constraints

The operational constraint for SOP is as follows:

$$P_i^{sop} + P_j^{sop} = 0 \quad i, j \in \Omega_n \tag{12}$$

$$-Q_i^{sop,\max} \le Q_i^{sop} \le Q_i^{sop,\max} \quad i \in \Omega_n \tag{13}$$

$$\sqrt{(P_i^{sop})^2 + (Q_i^{sop})^2} \le S^{sop} \quad i \in \Omega_n \tag{14}$$

where P_i^{sop} and P_j^{sop} denote the active power flowing through the SOP terminals located at nodes i and j; $Q^{sop,\max}$ indicates the SOP's maximum reactive power capacity. S^{sop} denotes the rated capacity of the SOP.

Additionally, the constraints (14) can be linearized through the inscribed polygons [9],

$$a_j P_i^{sop,pv} + b_j Q_i^{sop,pv} + c_j S^{sop,pv} \le 0 \quad j \in \{1,2,...,12\} \tag{15}$$

The structure of the distribution network can be expressed as:

$$\begin{aligned} \sum_{ij\in\Omega_b} \left(P_{t,ij} - r_{ij} l_{t,ij} \right) + P_{t,i} &= \sum_{jk\in\Omega_b} P_{t,jk} \\ \sum_{ij\in\Omega_b} \left(Q_{t,ij} - x_{ij} l_{t,ij} \right) + Q_{t,i} &= \sum_{jk\in\Omega_b} Q_{t,jk} \end{aligned} \tag{16}$$

$$V_{t,i} - V_{t,j} - 2\left(r_{ij} P_{t,ij} + x_{ij} Q_{t,ij} \right) = 0 \tag{17}$$

where $P_{t,ij}$ and $Q_{t,ij}$ denote the active and reactive power flow of branch ij , respectively. r_{ij} and x_{ij} represent their resistance and reactance; and $V_{t,ij}$ corresponds to the voltage magnitudes.

Moreover, recognizing that extreme natural disasters can significantly alter network topology, branch outage indicators $\delta_{i,j}$ are introduced to update the branch power flow accordingly.

$$M(\delta_{ij} - 1) \le P_{ij} \le M(1 - \delta_{ij}) \tag{18}$$

$$M(\delta_{ij} - 1) \le Q_{ij} \le M(1 - \delta_{ij}) \tag{19}$$

Extreme natural disasters, such as extreme cold or heat, can significantly affect loads. Thus, the node load can be adjusted as follows:

$$P_{ij,s} = P_{ij,s}^{\mathrm{base}} + P_{ij,s}^{\mathrm{inc}} \tag{20}$$

where $P_{ij,s}^{\mathrm{base}}$ denotes the load demand under typical scenarios, and $P_{ij,s}^{\mathrm{inc}}$ represents the incremental load demand resulting from extreme natural disasters, calculated based on [8].

C. Unified Climate Impact Model

Distribution networks frequently face various extreme natural disasters during operation stage, resulting in time-consuming repeated assessments of their impact on power systems at the operational stage. To efficiently address these complexities, this study proposes a generalized climate impact method capable of simultaneously capturing the effects of multiple extreme natural disasters scenarios.

$$f\left(\boldsymbol{B}, \boldsymbol{D}, p_k, \boldsymbol{x_k}\right) = 0 \tag{21}$$

where $\boldsymbol{B}$, $\boldsymbol{D}$, p_k, and $\boldsymbol{x_k}$ refer to the basic attributes, direct attributes, extreme natural disasters scenario weights, and the state variables of system components, respectively.

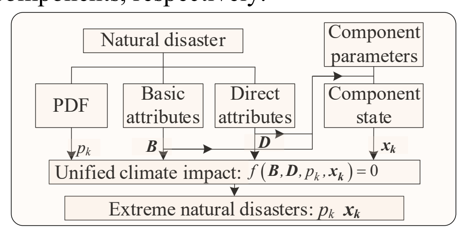

Figure 3. The proposed unified climate impact model

Basic attributes $\boldsymbol{B}$ characterize the occurrence and operational features of extreme weather events. For instance, in the case of typhoon events, these attributes include factors such as landfall location, trajectory, central pressure difference, and movement speed. The direct attributes $\boldsymbol{D}$ represent the intensity of extreme weather events, such as the magnitude of an earthquake. Due to the inherent uncertainty of extreme weather events, extreme weather scenario weights p_k are assigned to each scenario of a specific disaster type. [10].

Based on the unified climate impact model, we construct an uncertainty set (22). Γ_B is the uncertainty adjustment parameter for basic attributes, and Γ_D is the uncertainty adjustment parameter for direct attributes.

$$\sum_{s\in\Omega_s} B_s \le \Gamma_B \quad \sum_{s\in\Omega_s} D_s \le \Gamma_D \tag{22}$$

III. The Extended MIL-Shaped Algorithm

In summary, the entire hierarchical collaborative optimization model can be concisely expressed in matrix form as shown in (23). The proposed extended MIL-shaped algorithm is illustrated through (23).

$$\begin{aligned} \min\ & \boldsymbol{d_m}^{\boldsymbol{T}} \boldsymbol{x}_m + \boldsymbol{f_m}^{\boldsymbol{T}} \boldsymbol{y}_m + \max_{\boldsymbol{u}\in U} \min_{\boldsymbol{x}_l\in\mathbf{Z}, \boldsymbol{y}_l\in\mathbf{R}} \boldsymbol{d_l}^{\boldsymbol{T}} \boldsymbol{x}_l + \boldsymbol{f_l}^{\boldsymbol{T}} \boldsymbol{y}_l \\ \text{s.t.}\ & \boldsymbol{A}_m \boldsymbol{x}_m + \boldsymbol{B}_m \boldsymbol{y}_m \le \boldsymbol{b} \\ & \boldsymbol{D}\boldsymbol{x}_l + \boldsymbol{F}\boldsymbol{y}_l \le \boldsymbol{g} - \boldsymbol{G}_1 \boldsymbol{x}_m - \boldsymbol{G}_2 \boldsymbol{y}_m - \boldsymbol{H}\boldsymbol{u} \end{aligned} \tag{23}$$

where $\boldsymbol{x}_m$ and $\boldsymbol{y}_m$ represent the upper-level decision variables; $\boldsymbol{u}$ denotes the uncertainty variables associated with extreme

979-8-3315-8138-1

scenarios; $\boldsymbol{x}_l$ and $\boldsymbol{y}_l$ represent the lower-level decision variables. This forms a large-scale mixed-integer linear robust optimization model. This paper extends the optimality cut form of the traditional L-shaped algorithm [4] and proposes a MIL-shaped method to solve the problem.

In the *it* iteration, given the decision vector $\boldsymbol{x}_m^{it*}$, $\boldsymbol{y}_m^{it*}$, and $\boldsymbol{u}^{it*}$, the lower-level model is expressed as (24)

$$\begin{aligned} &\min_{\boldsymbol{x}_l \in \mathbf{Z}, \boldsymbol{y}_l \in \mathbf{R}} \boldsymbol{d}_l^{\boldsymbol{T}} \boldsymbol{x}_l + \boldsymbol{f}_l^{\boldsymbol{T}} \boldsymbol{y}_l \\ &\text{s.t. } \boldsymbol{D}\boldsymbol{x}_l + \boldsymbol{F}\boldsymbol{y}_l \le \boldsymbol{g} - \boldsymbol{G}_1 \boldsymbol{x}_m^{it*} - \boldsymbol{G}_2 \boldsymbol{y}_m^{it*} - \boldsymbol{H}\boldsymbol{u}^{it*} \end{aligned} \tag{24}$$

By substituting the optimal solutions $\boldsymbol{x}_l$ and $\boldsymbol{y}_l$ into the unified climate impact model and introducing slack variables θ^{it}, we generate the dual slack problem of lower-level subproblems, as shown in (25).

$$\begin{aligned} &\max_{\theta \in \mathbf{R}\ \boldsymbol{u} \in U} \theta^{it} \\ &\text{s.t. } \theta \le \boldsymbol{f}_l^{\boldsymbol{T}} \boldsymbol{y}_l^{it} + (\boldsymbol{g} - \boldsymbol{F}\boldsymbol{y}_l^{it} - \boldsymbol{G}_1 \boldsymbol{x}_m^{it*} - \boldsymbol{G}_2 \boldsymbol{y}_m^{it*} - \boldsymbol{H}\boldsymbol{u}^{it*})\boldsymbol{\pi}_1^{it} \\ &\quad \boldsymbol{D}\boldsymbol{\pi}^{it} \le \boldsymbol{d}_l,\ \boldsymbol{\pi}_1^{it} \in \mathbf{R}_+ \end{aligned} \tag{25}$$

where $\boldsymbol{\pi}_1^{it}$ represents the dual variable of $\boldsymbol{x}_l$. The optimal solution $\boldsymbol{\pi}_1^{it*}$ and $\boldsymbol{y}_l^*$ can be obtained through solving (25). Following this, the upper-level model is reformulated as:

$$\begin{aligned} &\min \boldsymbol{d}_m^{\boldsymbol{T}} \boldsymbol{x}_m + \boldsymbol{f}_m^{\boldsymbol{T}} \boldsymbol{y}_m + \theta \\ &\text{s.t. } \boldsymbol{A}_m \boldsymbol{x}_m + \boldsymbol{B}_m \boldsymbol{y}_m \le \boldsymbol{b} \\ &\quad \boldsymbol{E}_{it} \boldsymbol{x}_m + \boldsymbol{K}_{it} \boldsymbol{y}_m + \theta \ge \boldsymbol{e}_{it} \end{aligned} \tag{26}$$

The constraint $\boldsymbol{E}_{it} \boldsymbol{x}_m + \boldsymbol{K}_{it} \boldsymbol{y}_m + \theta \ge \boldsymbol{e}_{it}$ represents the optimal cut, which is mathematically explained in [4]. Based on this foundation, we derive the mixed-integer optimal cut expression and extend the L-shaped method to address mixed-integer robust optimization problems, as shown in (27).

$$\begin{aligned} e_{it} &= \sum p_s (\boldsymbol{\pi}^*)^T (\boldsymbol{g} - \boldsymbol{G}_1 \boldsymbol{x}_m^* - \boldsymbol{G}_2 \boldsymbol{y}_m^* - \boldsymbol{H}\boldsymbol{u}^*) \\ \boldsymbol{E}_{it} &= \sum p_s (\boldsymbol{\pi}_1^{it*})^T \boldsymbol{G}_1 \\ \boldsymbol{K}_{it} &= \sum p_s (\boldsymbol{\pi}_2^{it*})^T \boldsymbol{G}_2 \end{aligned} \tag{27}$$

The variable $\boldsymbol{\pi}^*$ is determined by solving subproblems based on the unified climate impact model. $\boldsymbol{\pi}_2^{it*}$ represents the dual variable of $\boldsymbol{y}_l$ in iteration process *it*. Finally, by integrating (27) back into the master problem, the BMILP model is solved iteratively.

The convergence criterion for the proposed algorithm can be expressed as,

$$\theta^{it} \ge e_{it} - \boldsymbol{E}_{it} \boldsymbol{x}_m^{it} - \boldsymbol{K}_{it} \boldsymbol{y}_m^{it} \tag{28}$$

practical guarantees on solution optimality and convergence behavior, as detailed in [12].

IV. Case Study and Analysis

A. System configurations

In this section, we validate the proposed hierarchical collaborative optimization model and the extended MIL-shaped algorithm using a real distribution network, as shown in Fig. 4. The system consists of 30 buses and lines and is vulnerable to two types of extreme natural disasters: typhoons and earthquakes, with parameters detailed in [10]. The steel plant is located at node 15. The daily steel delivery quantity is set at 50 tons. Two SOPs are set up, connecting nodes 11 and 26, and nodes 6 and 21. Additionally, two PV units and two BS units are included in the case study, as shown in Fig. 4. The parameters are provided in Table I. The simulation was run on a standard PC equipped with an Intel Core 12700 CPU and 128.0 GB RAM. Gurobi version 10.0 was used in the study. The uncertainty adjustment parameter Γ_B for basic attributes is 12, and the uncertainty adjustment parameter Γ_D for direct attributes is 6. Taking a typhoon event as an example, a 24-hour disruption duration is assumed, and the optimization is performed on an hourly basis.

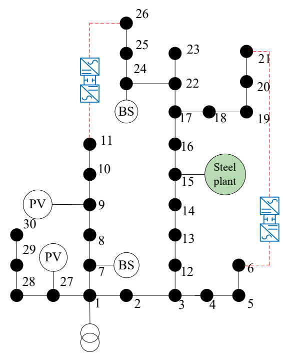

Figure 4. The Topology of the test system

To validate the proposed method, four comparison scenarios are set up, as presented in Table II.

TABLE I. Parameters of DGs

	BS unit (kWh)		PV unit (kW)	
Location	7	24	9	27
Capacity	400	300	300	500

TABLE II. Scenario configuration

Case	SOP	SPDR
Scenario 1	N	N
Scenario 2	Y	N
Scenario 3	N	Y
Scenario 4	Y	Y

TABLE III. Economic Analysis

Case	Operation cost ($\times 10^3$\$)	Load shedding cost ($\times 10^3$\$)
Scenario 1	3.59	68.16
Scenario 2	4.73	53.48
Scenario 3	4.83	50.67
Scenario 4	6.01	31.29

TABLE IV. Comparison of Load Shedding

	Scenario			
	1	2	3	4
Load shedding (MWh)	17.04	13.37	12.67	7.82
Load shedding rate (%)	27.29	21.41	20.29	12.52

B. Analysis of hierarchical collaborative optimization model

Table III summarizes the optimization results under four different scenarios. In Scenario 1, neither SOP nor steel plant load management is applied, resulting in the lowest operational cost but also the highest load shedding cost of \$68.16×10[3]. Scenarios 2 and 3 separately incorporate SOP and steel plant load management, reducing the load-shedding costs to \$53.48×10[3] and \$50.67×10[3], respectively, while incurring additional operational costs of \$1.14×10[3] and \$1.24×10[3]. Finally, Scenario 4 combines both SOP and steel plant load management, resulting in the highest operational cost of \$6.01×10[3], yet significantly decreasing load shedding cost to \$31.29×10[3]. Notably, this reduction exceeds the combined reductions achieved in Scenarios 2 and 3 individually, indicating a synergistic effect between SOP and load management strategies.

Table IV further compares the load shedding amounts across the four scenarios. It is evident that through the collaborative optimization of SOP and steel plant load management, the load shedding value can be reduced by 54.11%.

TABLE V. DEMAND RESPONSE CAPABILITY OF VARIOUS PROCESSES

Process	Coking	EAF	Sintering	Pelletizing	BF	BOF	Rolling
Demand response power (kWh)	32.3	676.4	67.0	81.5	62.6	86.3	236.5

Taking Scenario 4 as an example, the demand response potential of various processes is further analyzed. Table V shows the distribution of demand response power across various processes in the steel plant. Overall, the steel plant can provide a total demand response capacity of 1242.6 kWh, accounting for approximately 6.21% of its total electricity consumption. Specifically, due to its electric-driven nature and operational flexibility, the EAF process exhibits the highest demand response capacity of 676.4 kWh, accounting for 54.43% of the total. In contrast, the BF and BOF processes, characterized by continuous operation, temperature stability requirements, and lower electricity dependency, offer relatively limited flexible response capacities. Additionally, the rolling process, involving shaping and rolling of steel products, can flexibly adjust its operations according to external electricity demand, providing up to 236.5 kWh of adjustable load.

C. Efficiency of the extended MIL-shaped algorithm

To validate the efficiency of the extended MIL-shaped algorithm, a comparison is made with the Nest-C&CG method [11]. After both algorithms converge, the optimization results, as shown in Table III, demonstrate that the proposed algorithm converges to a consistent optimal value.

TABLE VI. COMPARISON OF THE PERFORMANCE

Method	Solving Time (s)			
	Scenario 1	Scenario 2	Scenario 3	Scenario 4
Nest-C&CG	32.14	44.59	41.37	48.53
MIL-shaped	24.68	32.14	32.51	35.68

Table VI compares the solving times for four scenarios using two methods: Nest-C&CG and MIL-shaped. The proposed MIL-shaped method consistently outperforms Nest-C&CG, with a reduction in solving time for all scenarios. For example, in Scenario 1, the MIL-shaped method is 7.46 s faster than Nest-C&CG. Similar improvements are observed in the other scenarios, highlighting the MIL-shaped method's superior computational efficiency.

TABLE VII. COMPUTATIONAL EFFICIENCY OF DIFFERENT NETWORKS

Method	Solving Time (s)		
	30 bus	33 bus	69 bus
Nest-C&CG	48.53	50.32	93.74
MIL-shaped	35.68	35.94	68.58

V. CONCLUSIONS

This study proposes a hierarchical collaborative optimization model that integrates steel plant demand response and SOP. The model is formulated as a bilevel mixed-integer programming problem. Furthermore, considering that a single region may be affected by multiple types of extreme natural disasters, a unified climate impact model is developed. To accelerate the solution process, an extended MIL-shaped algorithm is developed for efficiently solving the proposed hierarchical optimization model. A real-case study demonstrates that the proposed hierarchical collaborative model reduces load shedding by more than 54%. In addition, numerical results confirm that the extended MIL-shaped algorithm significantly improves computational efficiency compared with the nested C&CG method.

REFERENCES

[1] H. Hou, J. Tang, Z. Zhang, et al., "Resilience enhancement of distribution network under typhoon disaster based on two-stage stochastic programming," *Appl. Energy*, vol. 338, pp. 120892, 2023.

[2] X. Zhang, G. Hug, Z. Kolter, et al., "Industrial demand response by steel plants with spinning reserve provision," in *Proc. 2015 North Amer. Power Symp. (NAPS)*, 2015, pp. 1–6.

[3] C. Tian, J. Li, C. Wang, et al., "Demand response strategy considering industrial loads and energy storage with high proportion of wind-power integration," *Sensors*, vol. 24, no. 22, pp. 7335, 2024.

[4] P. Fan, T. Yu, Z. Wang, et al., "Resilience-oriented soft open point deployment with topology-variable-based frequency stability constraints for distribution networks," *Appl. Energy*, vol. 394, pp. 126120, 2025.

[5] K. Wang, Y. Xue, Y. Zhou, et al., "Distributed coordinated reconfiguration with soft open points for resilience-oriented restoration in integrated electric and heating systems," *Appl. Energy*, vol. 365, pp. 123207, 2024.

[6] Van Slyke R M, Wets R. "L-Shaped Linear Programs with Applications to Optimal Control and Stochastic Programming." *SIAM Journal on Applied Mathematics*, vol. 17, no. 4, pp. 638–663, July. 1969.

[7] Low S H. "Convex Relaxation of Optimal Power Flow—Part I: Formulations and Equivalence." *IEEE Trans. Control of Network Systems*, vol. 1, no. 1, pp. 15–27, Mar. 2014.

[8] J. Bai, et al., "A weather-induced power load forecasting method based on asymmetric single valley curves," in *Proc. 2nd Asian Conf. on Frontiers of Power and Energy (ACFPE)*, 2023, pp. 399–405.

[9] S. Wang, S. Chen, L. Ge, and L. Wu, "Distributed generation hosting capacity evaluation for distribution systems considering the robust optimal operation of OLTC and SVC." *IEEE Trans. Sustain. Energy*, vol. 7, no. 3, pp. 1111–1123, Jul. 2016.

[10] Wang H, Hou K, Zhao J, et al. "Planning-Oriented Resilience Assessment and Enhancement of Integrated Electricity-Gas System Considering Multi-Type Natural Disasters." *Applied Energy*, vol. 315, pp. 118824, June. 2022.

[11] H. Qiu, W. Gu, Y. Xu, et al. "Interval-partitioned uncertainty constrained robust dispatch for AC/DC hybrid microgrids with uncontrollable renewable generators." *IEEE Trans. Smart Grid*, vol. 10, no. 4, pp. 4603–4614, Jul. 2019.

[12] J. Qu *et al.*, "Enhancing distribution network resilience: A multi-level cooperative planning approach for hydrogen-electrical microgrids and SOP," in *Proc. 2024 IEEE Power & Energy Society General Meeting (PESGM)*, 2024.

979-8-3315-8138-1